Evaluating a high-resolution urban fossil CO2 emissions inventory using eddy-covariance flux measurements and source partitioning

Kai Wu[1], Kenneth J. Davis[2], Natasha L. Miles[2], Scott J. Richardson[2], Thomas Lauvaux[3], Daniel Sarmiento[2], Nikolay Balashov[4], Klaus Keller[2], Jocelyn Christine Turnbull[5], Kevin Robert Gurney[6], Jianming Liang[7], and Geoffrey S Roest[6]

[1]University of Edinburgh
[2]Pennsylvania State University
[3]2Laboratoire des Sciences du Climat et de l'Environnement
[4]NASA Goddard Space Flight Center
[5]GNS Science
[6]Northern Arizona University
[7]Arizona State University

November 21, 2022

Abstract

We present the first quantitative comparison of source-partitioned CO2 flux measurements with a high-resolution urban fossil CO2 emissions inventory. We use tower-based measurements of CO and 14C to partition net CO2 flux measurements into fossil and biogenic components in a suburban environment. A flux footprint model is used to quantify spatial patterns in fluxes. The partitioned fossil CO2 emissions are compared to a 200-m resolution emissions inventory (Hestia). The results indicate that Hestia and the partitioned flux data agree remarkably well on a seasonal average scale. The Hestia inventory is biased by 3.2% (cold season) and 9.1% (warm season). Their temporal-spatial patterns match closely. In addition, biogenic CO2 uptake is 25% of local fossil emissions during afternoon in the cold season. This work demonstrates the effectiveness of using eddy-covariance flux measurements both for evaluating urban emissions inventories and for quantifying urban ecosystem fluxes.

Evaluating a high-resolution urban fossil CO_2 emissions inventory using eddy-covariance flux measurements and source partitioning

Kai Wu[1,*], Kenneth J. Davis[1,2], Natasha L. Miles[1], Scott J. Richardson[1], Thomas Lauvaux[3], Daniel P. Sarmiento[4], Nikolay V. Balashov[4], Klaus Keller[5,2], Jocelyn Turnbull[6,7], Kevin R. Gurney[8,9], Jianming Liang[9], Geoffrey Roest[8]

[1]Department of Meteorology and Atmospheric Science, The Pennsylvania State University, University Park, Pennsylvania 16802, United States
[2]Earth and Environmental Systems Institute, The Pennsylvania State University, University Park, Pennsylvania 16802, United States
[3]Laboratoire des Sciences du Climat et del'Environnement, CEA, CNRS, UVSQ/IPSL, Université Paris-Saclay, Orme des Merisiers, 91191 Gif-sur-Yvette Cedex, France
[4]NASA Goddard Space Flight Center, Greenbelt, Maryland 20771, United States
[5]Department of Geosciences, The Pennsylvania State University, University Park, Pennsylvania 16802, United States
[6]Rafter Radiocarbon Laboratory, GNS Science, Lower Hutt 5040, New Zealand
[7]CIRES, University of Colorado at Boulder, Boulder, Colorado 80309, United States
[8]School of Informatics, Computing and Cyber Systems, Northern Arizona University, Flagstaff, Arizona 85287, United States
[9]School of Life Sciences, Arizona State University, Tempe, Arizona 85281, United States
*now at: School of GeoSciences, The University of Edinburgh, Edinburgh, United Kingdom

Key Points:

- Urban CO_2 flux measurements are partitioned into fossil and biogenic components using CO and ^{14}C measurements and a flux-gradient method.
- The partitioned fossil CO_2 emissions show remarkable consistency of the comparison with an emissions inventory in time and space.
- Biogenic CO_2 fluxes within the city are non-negligible in the cold season and need to be considered in urban CO_2 monitoring.

Corresponding author: Kai Wu, kwu2@ed.ac.uk

Abstract

We present the first quantitative comparison of source-partitioned CO_2 flux measurements with a high-resolution urban fossil CO_2 emissions inventory. We use tower-based measurements of CO and ^{14}C to partition net CO_2 flux measurements into fossil and biogenic components in a suburban environment. A flux footprint model is used to quantify spatial patterns in fluxes. The partitioned fossil CO_2 emissions are compared to a 200-m resolution emissions inventory (Hestia). The results indicate that Hestia and the partitioned flux data agree remarkably well on a seasonal average scale. The Hestia inventory is biased by 3.2% (cold season) and 9.1% (warm season). Their temporal-spatial patterns match closely. In addition, biogenic CO_2 uptake is 25% of local fossil emissions during afternoon in the cold season. This work demonstrates the effectiveness of using eddy-covariance flux measurements both for evaluating urban emissions inventories and for quantifying urban ecosystem fluxes.

Plain Language Summary

This work presents the first comparison of two innovative approaches for quantifying urban CO_2 emissions from the combustion of fossil fuels. Both approaches can quantify emissions from neighborhoods with hourly time resolution. These methods show very similar results concerning the seasonal-mean fossil CO_2 emissions, as well as the emissions variation in time and space. We also find relatively large biological CO_2 exchange, even during winter when the biosphere is often assumed to be dormant. The results show great promise for these new methods of quantifying source, space and time resolved CO_2 exchanges, and emphasize the need to take biological CO_2 fluxes into account when attempting to quantify fossil CO_2 emissions using atmospheric measurements.

1 Introduction

Cities are becoming the focus for formulating and implementing carbon dioxide (CO_2) emissions mitigation efforts (Hutyra et al., 2014; Lee & Koski, 2014; Bulkeley, 2013). Evaluating the effectiveness of emissions reduction efforts requires accurate and independent CO_2 emissions estimates (Lauvaux et al., 2020; Turnbull et al., 2018). Although cities cover only 3% of the global land area, urban areas are home to 55% of the world's population, a proportion that is expected to increase to 68% by 2050 (Chaouad & Verzeroli, 2018). Overall, more than 70% of global fossil fuel CO_2 (CO_2ff) emissions are from urban areas (Edenhofer et al., 2015). Efforts to assess and mitigate CO_2 emissions can provide benefits for urban sustainability and balanced economic growth (Hsu et al., 2019).

Urban areas are consistently reported as a net source of CO_2 (Velasco & Roth, 2010). The temporal variation of urban CO_2 is dependent on human activities and urban ecosystems (McKain et al., 2012; Pataki et al., 2006). The eddy-covariance technique has been applied to measure urban CO_2 emissions for about two decades. This method has been demonstrated in many cities (Björkegren & Grimmond, 2018; Ao et al., 2016; Lietzke et al., 2015; Järvi et al., 2012; Christen et al., 2011; Vogt et al., 2006; Nemitz et al., 2002; Grimmond et al., 2002). The attribution of urban CO_2 flux measurements is challenging due to the spatial heterogeneity, mixed emission sources and sinks, and limited spatial coverage of flux measurements (Aubinet et al., 2012). Although most of urban flux studies focus on the total observed CO_2 flux, a few studies attempt to partition net flux measurements into fossil and biogenic components accounting for the temporal and spatial variability of the multiple sources and sinks. Menzer and McFadden (2017) modeled fossil CO_2 emissions based on winter data and extrapolated them to the growing season to estimate biogenic fluxes. Ishidoya et al. (2020) demonstrated partitioning of CO_2 fluxes into liquid and gaseous fossil fuel components using O_2 and CO_2 measurements.

Sugawara et al. (2021) used a nearby tower to estimate the biogenic component of a total CO_2 flux measurement.

Quantification of anthropogenic CO_2 emissions is challenging due to the difficulty of separating CO_2ff emissions from biogenic CO_2 (CO_2bio) fluxes (Miller et al., 2020; Basu et al., 2020; Menzer & McFadden, 2017; Pataki et al., 2007). Previous studies have demonstrated the feasibility of using ^{14}C isotope measurements to separate CO_2ff from CO_2bio fluxes (Basu et al., 2016; Turnbull et al., 2015; Miller et al., 2012), but flask measurements of ^{14}C are expensive and discontinuous. Continuous measurements of carbon monoxide (CO) provide another approach to track CO_2ff emissions (Silva et al., 2013; Levin & Karstens, 2007; Turnbull et al., 2006). Uncertainties in the CO to CO_2ff ratio, which vary as a function of emission sectors, complicate the attribution of urban CO_2 fluxes. These methods have not yet been applied to eddy-covariance flux measurements.

Emissions inventories use activity data to aggregate source-specific and total emissions (Boden et al., 2009; Gurney et al., 2009; Olivier & Janssens-Maenhout, 2012), but the differences among inventories are sizeable (Gately & Hutyra, 2017; Oda et al., 2019). Atmospheric inversions use inventories as prior estimates of emissions and optimize the emissions using atmospheric mole fraction observations (Bréon et al., 2015; Turner et al., 2016; Staufer et al., 2016; Lauvaux et al., 2016; Kunik et al., 2019; Lauvaux et al., 2020). Determination of the uncertainty in the inversion results hinges on estimates of errors in atmospheric transport models (Deng et al., 2017; Sarmiento et al., 2017) and emissions inventories (Wu et al., 2018). The Hestia emissions inventory (Gurney et al., 2012) was developed in part to support the Indianapolis Flux Experiment (INFLUX) and uses energy consumption, population density, and traffic data to quantify CO_2ff emissions for an entire urban landscape at an approximately 200-m and hourly resolution. The high-resolution performance of the Hestia inventory has not yet been evaluated using atmospheric observations.

This study compares seven months of source-partitioned CO_2 eddy-covariance flux measurements with a high-resolution emissions inventory (Hestia) in a suburban region of Indianapolis, Indiana, USA. We partition the total CO_2 flux measurements into CO_2ff and CO_2bio components using a flux-gradient relationship (Stull, 2012; Ishidoya et al., 2020) and atmospheric CO measurements. ^{14}C isotope measurements are used to estimate the CO to CO_2ff ratio and reduce the uncertainty in the flux decomposition. Our source decomposition methods are similar to those used by Ishidoya et al. (2020) and Sugawara et al. (2021). In addition, we use a flux footprint model (Kljun et al., 2015, 2004) to match each flux measurement in space and time with the Hestia inventory to provide a direct comparison of independent estimates of fossil CO_2 emissions at high spatial and temporal resolution. This is, to our knowledge, the first such comparison of these innovative and independent assessments of high-resolution urban CO_2 emissions, and is timely given the growing interest in studies of urban systems.

2 Data and Methods

2.1 Site Descriptions and Atmospheric CO_2 Flux Measurements

The INFLUX observation network (Davis et al., 2017) measures atmospheric CO_2 and CO mole fractions, and net CO_2 fluxes in and around Indianapolis, IN (Figure 1). The locations, sampling heights and measurements at these sites are described by Miles et al. (2017) and instrument performance by Richardson et al. (2017). ^{14}C isotope measurements, which are related to CO_2ff emissions, are collected weekly using a flask sampling system (Turnbull et al., 2015). We focus on seven months (January to July, 2013) of eddy-covariance flux measurements at Tower 2 located in a heterogeneous suburban environment (Figures 1 and S1). There is a highway to the north, urban vegetation to the south, and neighborhoods with detached houses. The heterogeneous surroundings

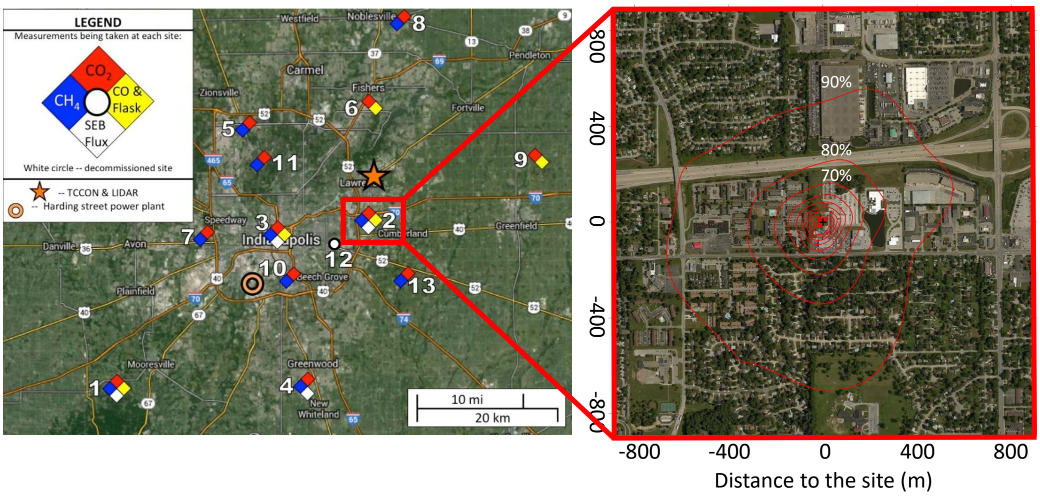

Figure 1. The Indianapolis Flux Experiment (INFLUX) measurement network in Indianapolis, IN (left) and cumulative flux footprints from January to July in 2013 at Tower 2 (right). The contours in the right panel represent the percentage of the time-integrated flux that comes from within that boundary. The color of the marker in the left panel represents the measurements at each site: red for CO_2, yellow for CO and ^{14}C, blue for CH_4, and white for surface energy balance fluxes. The coordinates in the right panel are the distance (m) to the measurement site.

present a good test of our ability to partition net CO_2 flux measurements into biogenic and fossil fuel components.

The flux instrumentation, which includes a sonic anemometer (Campbell Scientific, CSAT-3) and a high-frequency open-path infrared CO_2 sensor (LI-COR Environmental, LI-7500), is mounted at 30 m above ground level (AGL) on Tower 2. The eddy-covariance technique measures the covariance between fluctuations in vertical wind velocity and CO_2 density to detect the integrated exchange of CO_2 between land and atmosphere (Lee et al., 2004; Foken & Napo, 2008; Aubinet et al., 2012). We use flux calculation and filtering methods recommended by Vickers and Mahrt (1997). We filter out extreme values outside 3.5 σ range of the data (0.2% of data are filtered out) and nighttime fluxes during weak turbulence conditions when the friction velocity is less than 0.2 m/s (3.6% of data are filtered out) (Gu et al., 2005). Negative fluxes confirm the predominant role of photosynthesis from the urban vegetation around this site (Figure S2). We define the cold season as January to March (JFM) and the warm season as April to July (AMJJ) based on the presence of negative total CO_2 fluxes during the daytime in the warm season (Figure S3).

2.2 Partitioning Fossil Fuel and Biogenic CO_2 Fluxes

To partition fossil fuel and biogenic components from the net CO_2 flux measurements, we apply a flux-gradient method and atmospheric CO measurements. We measure CO_2 and CO mole fractions at 10 m and 40 m heights AGL at Tower 2 (Miles et al., 2017). We use the eddy-covariance flux measurement and measured vertical gradient in CO_2 to solve for the eddy diffusivity, and use that eddy diffusivity and the CO vertical gradient to solve for the CO flux, as shown in the supporting information. There are three assumptions in this method: (1) Turbulent eddies are small enough that local scalar gradients are proportional to turbulent fluxes; (2) CO and CO_2 are subject to the same vertical mixing processes; (3) Within the turbulent flux footprint, CO is mainly produced by fossil fuel combustion. We filter out counter-gradient fluxes, and limit the eddy diffusivity and CO flux within 3.5 σ range of their estimates to screen out extreme values caused by tiny denominators.

The emission ratio of CO to CO_2ff is estimated from flask measurements of ^{14}C and CO measurements (Turnbull et al., 2015). The urban CO enhancements are estimated by the differences between Tower 2 and upwind background sites (Tower 1 or 9 depending on the wind direction). The median and mean values of CO to CO_2ff ratios are 9.52 and 8.98 ppb ppm^{-1} (cold season) and 9.13 and 9.02 ppb ppm^{-1} (warm season) (Figure S4). We use 9 ppb ppm^{-1} as an approximate value to infer CO_2ff emissions. To test the uncertainty of using different ratios on the flux decomposition, we vary the emission ratio to 11 and 7 ppb ppm^{-1} based on the range of values estimated by Turnbull et al. (2015). Since traffic emissions are likely to have a higher ratio and residential emissions have a smaller ratio. We add another scenario with a CO to CO_2ff ratio of 15 ppb ppm^{-1} for northerly winds from the highway, and 7 ppb ppm^{-1} for the other wind directions.

2.3 Flux Footprint and Emissions Inventory

A flux footprint, which is defined as the contributing area upwind from the measurement site (Leclerc & Foken, 2014), is essential to account for the spatial heterogeneity of emission sources. We use a two-dimensional flux footprint model (Kljun et al., 2015, 2004) to match with the Hestia inventory. Tower-based measurements of wind field and boundary layer characteristics are used to estimate the input parameters of the footprint model (*i.e.* roughness length, Obukhov length, friction velocity, standard deviation of lateral velocity fluctuations, etc.). The size of footprint depends on measurement height, surface roughness, and atmospheric thermal stability. The footprint will increase with an increase in measurement height, with a decrease in surface roughness, and with an increase in atmospheric thermal stability (Burba & Anderson, 2010). The spatial resolution of the footprint model is approximately two meters. We match every flux footprint with Hestia via a convolution of the influence function with the Hestia emissions.

3 Results

Net CO_2 flux measurements, decomposed as a function of time and space, behave as expected given the environment surrounding the tower. Observed CO_2 emissions are larger in the cold season than the warm season (Figure 2a), perhaps due to increased emissions from building heating around the tower (Figures 1 and S1). In the cold season, there are two prominent peaks in emissions likely corresponding to peaks in traffic volume during rush hours. In the warm season, fossil fuel CO_2 emissions are mixed with photosynthesis and respiration from urban vegetation within the flux footprints. The daytime photosynthetic uptake of CO_2 indicates the role of urban vegetation. The spatial patterns of flux data show high emissions from the north, and lower emissions or net uptake from the south (Figures 2b and 2c), consistent with the highway to the north and urban vegetation to the south of the tower (Figures 1 and S1).

Partitioning of the net observed CO_2 fluxes into fossil and biogenic components yields broadly plausible temporal behavior of these flux components (Figure 3). While substantially smaller than the estimated CO_2ff emissions, the cold season CO_2bio uptake is 25% of urban CO_2ff emissions during the afternoon (Figure 3a), which is non-negligible and need to be considered to obtain accurate CO_2ff emissions. A typical pattern of ecosystem fluxes emerges in the warm season (Figure 3b). The warm season CO_2bio fluxes are equal in amplitude to the CO_2ff emissions, emphasizing the importance of accounting for CO_2bio fluxes in attempts to quantify urban CO_2ff emissions.

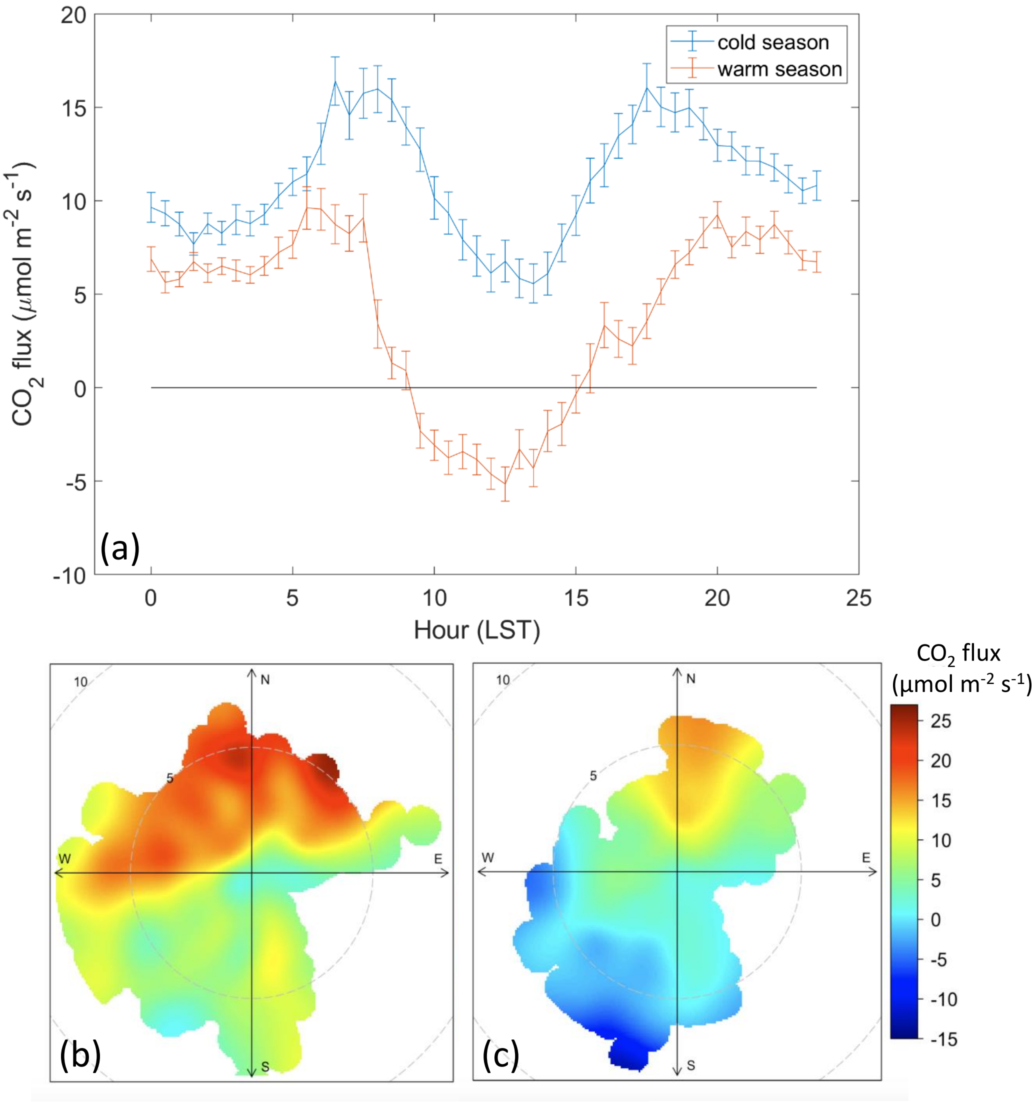

Figure 2. Diurnal variation of seasonally-averaged CO_2 flux measurements during the cold (JFM) and warm (AMJJ) seasons in 2013 (a). Error bars indicate the standard errors of the seasonal means. Spatial variation of time-averaged CO_2 fluxes in the cold (b) and warm (c) seasons. Color indicates flux magnitude. The radial coordinate corresponds to wind speed (m s^{-1}) and the polar coordinate defines wind direction.

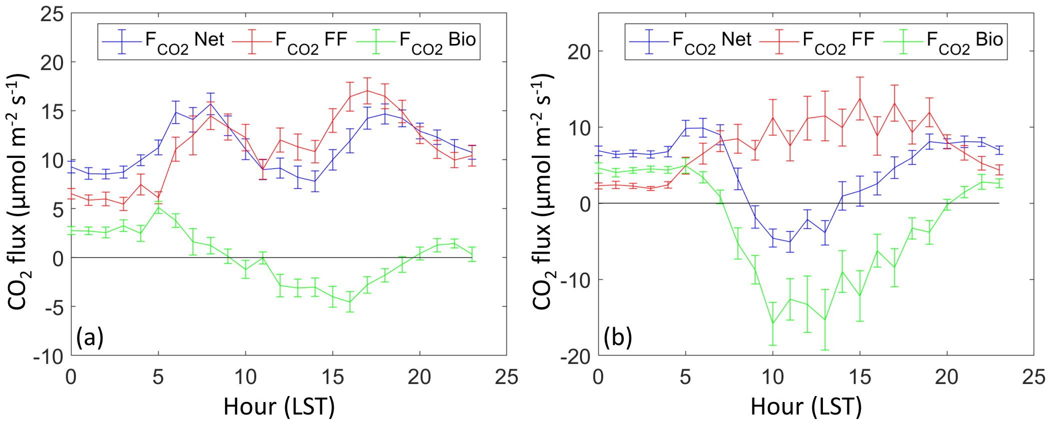

Figure 3. Diurnal variation of seasonally-averaged net CO_2 flux measurements (F_{CO2}Net) and the partitioned fossil fuel (F_{CO2}FF) and biogenic (F_{CO2}Bio) fluxes in the cold (JFM) (a) and warm (AMJJ) (b) seasons in 2013. Error bars are the standard errors of the seasonal means.

The seasonally-averaged eddy-covariance CO_2ff emissions estimates show remarkable similarity to the Hestia inventory when matched in space and time using flux footprints. Seasonal-mean CO_2ff emissions differ (Hestia minus OBS) by 0.36 μmol m^{-2} s^{-1} (3.2% of the mean partitioned CO_2ff emissions) in the cold season (Figure 4a) and 0.62 μmol m^{-2} s^{-1} (9.1% of the mean partitioned CO_2ff emissions) in the warm season (Figure 4b). The corresponding root mean square errors (RMSEs) are 8.91 μmol m^{-2} s^{-1} and 7.54 μmol m^{-2} s^{-1}, which include random measurement errors in the flux data.

The temporal patterns of seasonally-averaged Hestia and eddy-covariance CO_2ff emissions also agree remarkably well (Figures 4c and 4d). The correlation coefficients of the seasonal-mean diurnal variations are 0.86 (cold season) and 0.93 (warm season). The Hestia emissions are smaller during the night and higher during the day compared to the partitioned observations in the cold season (Figures 4c and S5a), and consistently slightly higher than the partitioned observations in the warm season (Figures 4d and S5b).

We also find consistency in the comparison of eddy-covariance and Hestia CO_2ff emissions as a function of wind direction (Figure S6 and Table 1). In the cold season, the Hestia emissions are higher than the observed CO_2ff emissions for all wind directions except the north, west and northwest wind (Table 1). A similar pattern exists in the warm season. Since residential buildings lie upwind in the west and northwest wind directions (Figures 1 and S1), we infer that residential emissions may be the source of this discrepancy.

These results are somewhat sensitive to the choice of CO to CO_2ff emission ratio in the flux decomposition. Seasonal-mean flux bias and bias percentage change significantly when the emission ratio varies from 9 ppb ppm^{-1} to 11 or 7 ppb ppm^{-1} (Table S1 and Figure S7a). The temporal variations are not highly sensitive to this choice (Figure S7b). The scenario with the space-varying emission ratio (15 & 7 ppb ppm^{-1}), which may be more realistic than a constant ratio, does not significantly change compared to the default scenario (9 ppb ppm^{-1}) either the comparison of the diurnal variation (Figure S7b) or the bias estimation (Table S1).

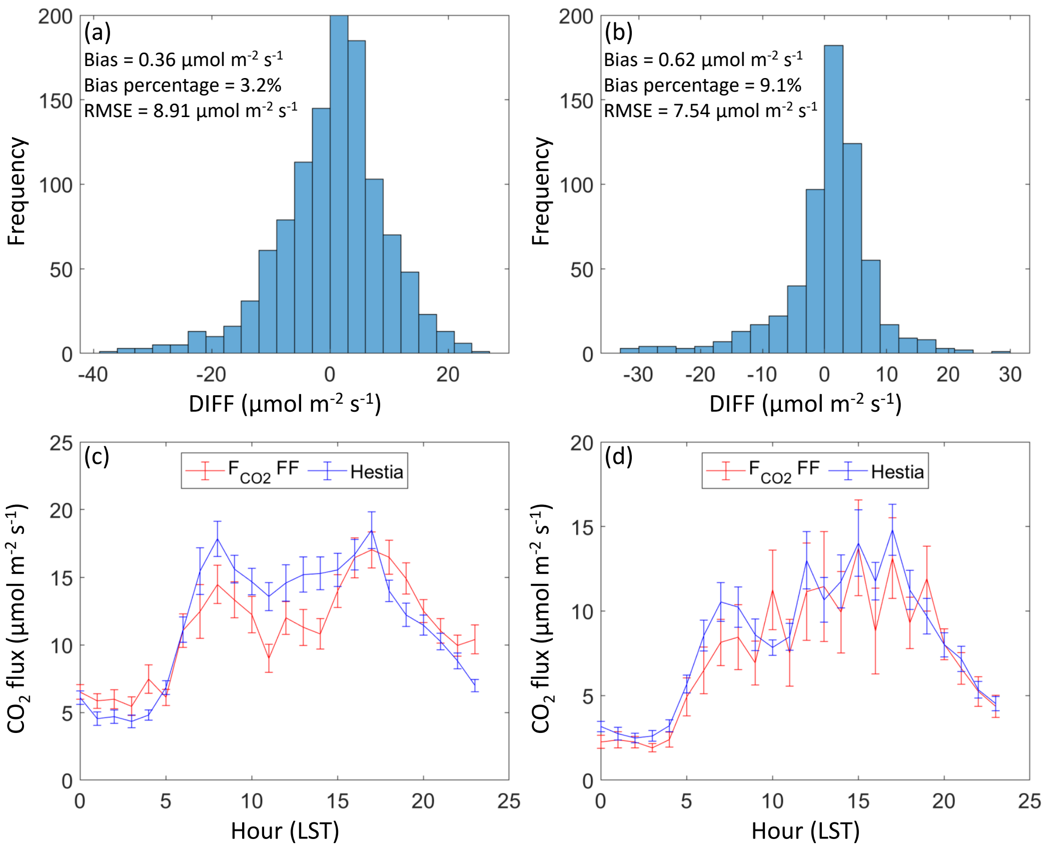

Figure 4. Histogram of flux differences between the Hestia inventory and the partitioned fossil fuel CO_2 emissions (Hestia minus OBS) in the cold (JFM) (a) and warm (AMJJ) (b) seasons in 2013. Bias, bias percentage compared to the mean partitioned CO_2ff emissions, and root mean square error (RMSE) are listed. Diurnal variation of seasonally-averaged CO_2ff emissions in the cold (c) and warm (d) seasons. Error bars are the standard errors of the seasonal means.

Table 1. Statistics of flux differences (μmol m^{-2} s^{-1}) between the Hestia inventory and the partitioned fossil fuel CO_2 emissions (Hestia minus OBS) for different wind directions.

	DIFF	N	NE	E	SE	S	SW	W	NW
Cold Season (JFM)	Median	-2.00	3.32	2.88	3.45	4.14	3.15	-4.47	-2.14
	Mean	-1.93	5.88	4.88	3.58	3.84	1.89	-4.72	-1.87
	RMSE[a]	10.98	9.27	8.22	5.63	7.45	8.00	10.40	9.06
Warm Season (AMJJ)	Median	2.49	3.34	1.92	1.98	0.98	0.42	-2.71	-4.27
	Mean	5.31	3.61	0.92	1.37	0.52	-1.32	-4.17	-5.21
	RMSE	8.24	9.32	5.19	5.54	5.97	8.62	8.47	13.66

[a]root mean square error

4 Conclusions and Discussion

The remarkably close agreement between the Hestia inventory and the partitioned eddy-covariance flux measurements suggests that both methods have the ability to quantify urban fossil CO_2 emissions. Neither approach has yet been cross-validated at such a high spatial and temporal resolution. The flux measurement partitioning is sensitive to the CO to CO_2ff emission ratio, but the consistency of Hestia and flux data suggests that flask measurements have accurately quantified that ratio. These results need to be tested at other locations and over different periods of time. The success of this test suggests that these eddy-covariance flux decomposition methods can be used to quantify source-specific CO_2 emissions of neighborhood-scale urban metabolic processes. Further the successful comparison to Hestia suggests that the algorithms and input data used in the inventory system are accurate and precise even down to the fine resolution of the eddy-covariance flux measurements.

This study also shows the promise of using this approach for studying urban ecosystem CO_2 fluxes. Previous work has suggested that the edges found in urban ecosystems lead to fundamentally different behavior of these ecosystems (Reinmann et al., 2020), but these findings are largely based on chamber-scale flux measurements. It is not clear whether or not, when upscaled to spatial domains that integrate across many edges such as a suburban forest, existing ecosystem models and model parameters will suffice in describing urban CO_2bio fluxes. Current ecosystem models used in urban studies are largely devoid of urban ecosystem flux measurements in either calibration or evaluation due to lack of data (Wu et al., 2021; Hardiman et al., 2017). We suggest that the decomposition methods can serve as a new approach for obtaining ecosystem flux data necessary to develop the next generation of urban ecosystem models.

Finally, this study emphasizes the importance of urban ecosystem fluxes, both in the growing/warm season and the dormant/cold season. The importance of these fluxes has been shown in multiple observational (Miller et al., 2020; Turnbull et al., 2015) and inversion (Lauvaux et al., 2020; Sargent et al., 2018; Wu et al., 2018) studies, but the impact of uncertain biological fluxes has been shown to be large (Lauvaux et al., 2020; Wu et al., 2018), and we have not had direct flux measurements available for evaluating the modeled ecosystem flux priors. Further, a number of studies (Lauvaux et al., 2016; Heimburger et al., 2017) have made the reasonable assumption of neglecting CO_2bio fluxes in the dormant season. This work shows that urban ecosystems in Indianapolis are moderately active even in the cold season. More urban flux measurements are needed to study the range of urban ecosystem CO_2 fluxes.

Conflict of Interest

The authors declare no competing interests.

Data Availability Statement

The Hestia inventory is available online (https://hestia.rc.nau.edu/), and other data used in this analysis are available on the INFLUX website (http://sites.psu.edu/influx/).

Acknowledgments

The authors thank Bernd J. Haupt (PSU) for data acquisition and quality control. This work was funded by the National Institute of Standards and Technology (Project 70NANB10H245). T. Lauvaux was supported by the French research program Make Our Planet Great Again (Project CIUDAD). K.R. Gurney, J. Liang, and G. Roest received support from the National Aeronautics and Space Administration (Grant NNX14AJ20G) and the National Institute of Standards and Technology (Grant 70NANB16H264N).

References

Ao, X., Grimmond, C., Chang, Y., Liu, D., Tang, Y., Hu, P., . . . Tan, J. (2016). Heat, water and carbon exchanges in the tall megacity of Shanghai: challenges and results. *International Journal of Climatology*, *36*(14), 4608–4624.

Aubinet, M., Vesala, T., & Papale, D. (2012). *Eddy covariance: a practical guide to measurement and data analysis*. Springer Science & Business Media.

Basu, S., Lehman, S. J., Miller, J. B., Andrews, A. E., Sweeney, C., Gurney, K. R., . . . Tans, P. P. (2020). Estimating US fossil fuel CO_2 emissions from measurements of ^{14}C in atmospheric CO_2. *Proceedings of the National Academy of Sciences*, *117*(24), 13300–13307.

Basu, S., Miller, J. B., & Lehman, S. (2016). Separation of biospheric and fossil fuel fluxes of CO_2 by atmospheric inversion of CO_2 and $^{14}CO_2$ measurements: observation system simulations. *Atmospheric Chemistry and Physics*, *16*(9), 5665–5683.

Björkegren, A., & Grimmond, C. (2018). Net carbon dioxide emissions from central London. *Urban Climate*, *23*, 131–158.

Boden, T. A., Marland, G., & Andres, R. J. (2009). Global, regional, and national fossil-fuel CO_2 emissions. *Carbon Dioxide Information Analysis Center, Oak Ridge National Laboratory, US Department of Energy, Oak Ridge, Tenn., USA*, *10*.

Bréon, F., Broquet, G., Puygrenier, V., Chevallier, F., Xueref-Remy, I., Ramonet, M., . . . others (2015). An attempt at estimating Paris area CO_2 emissions from atmospheric concentration measurements. *Atmospheric Chemistry and Physics*, *15*(4), 1707–1724.

Bulkeley, H. (2013). *Cities and Climate Change*. London: Routledge.

Burba, G., & Anderson, D. (2010). *A brief practical guide to eddy covariance flux measurements: principles and workflow examples for scientific and industrial applications*. Li-Cor Biosciences.

Chaouad, R., & Verzeroli, M. (2018). The urbanization of the world: Facts and challenges. *Revue internationale et strategique*(4), 47–65.

Christen, A., Coops, N., Crawford, B., Kellett, R., Liss, K., Olchovski, I., . . . Voogt, J. (2011). Validation of modeled carbon-dioxide emissions from an urban neighborhood with direct eddy-covariance measurements. *Atmospheric Environment*, *45*(33), 6057–6069.

Davis, K. J., Deng, A., Lauvaux, T., Miles, N. L., Richardson, S. J., Sarmiento, D. P., . . . others (2017). The Indianapolis Flux Experiment (INFLUX): a test-bed for developing urban greenhouse gas emission measurements. *Elem Sci Anth*, *5*.

Deng, A., Lauvaux, T., Davis, K. J., Gaudet, B. J., Miles, N., Richardson, S. J., . . . others (2017). Toward reduced transport errors in a high resolution urban CO_2 inversion system. *Elem Sci Anth*, *5*.

Edenhofer, O., et al. (2015). *Climate Change 2014: Mitigation of Climate Change* (Vol. 3). Cambridge University Press.

Foken, T., & Napo, C. J. (2008). *Micrometeorology*. Springer.

Gately, C., & Hutyra, L. (2017). Large uncertainties in urban-scale carbon emissions. *Journal of Geophysical Research: Atmospheres*, *122*(20), 11–242.

Grimmond, C., King, T., Cropley, F., Nowak, D., & Souch, C. (2002). Local-scale fluxes of carbon dioxide in urban environments: methodological challenges and results from Chicago. *Environmental Pollution*, *116*, S243–S254.

Gu, L., Falge, E. M., Boden, T., Baldocchi, D. D., Black, T., Saleska, S. R., . . . others (2005). Objective threshold determination for nighttime eddy flux filtering. *Agricultural and Forest Meteorology*, *128*(3-4), 179–197.

Gurney, K. R., Mendoza, D. L., Zhou, Y., Fischer, M. L., Miller, C. C., Geethakumar, S., & de la Rue du Can, S. (2009). High resolution fossil fuel combustion

CO_2 emission fluxes for the United States. *Environmental Science & Technology*, *43*(14), 5535–5541.

Gurney, K. R., Razlivanov, I., Song, Y., Zhou, Y., Benes, B., & Abdul-Massih, M. (2012). Quantification of fossil fuel CO_2 emissions on the building/street scale for a large US City. *Environmental Science & Technology*, *46*(21), 12194–12202.

Hardiman, B. S., Wang, J. A., Hutyra, L. R., Gately, C. K., Getson, J. M., & Friedl, M. A. (2017). Accounting for urban biogenic fluxes in regional carbon budgets. *Science of The Total Environment*, *592*, 366–372.

Heimburger, A. M., Harvey, R. M., Shepson, P. B., Stirm, B. H., Gore, C., Turnbull, J., . . . others (2017). Assessing the optimized precision of the aircraft mass balance method for measurement of urban greenhouse gas emission rates through averaging. *Elem Sci Anth*, *5*.

Hsu, A., Höhne, N., Kuramochi, T., Roelfsema, M., Weinfurter, A., Xie, Y., . . . others (2019). A research roadmap for quantifying non-state and subnational climate mitigation action. *Nature Climate Change*, *9*(1), 11–17.

Hutyra, L. R., Duren, R., Gurney, K. R., Grimm, N., Kort, E. A., Larson, E., & Shrestha, G. (2014). Urbanization and the carbon cycle: Current capabilities and research outlook from the natural sciences perspective. *Earth's Future*, *2*(10), 473–495.

Ishidoya, S., Sugawara, H., Terao, Y., Kaneyasu, N., Aoki, N., Tsuboi, K., & Kondo, H. (2020). O_2:CO_2 exchange ratio for net turbulent flux observed in an urban area of Tokyo, Japan, and its application to an evaluation of anthropogenic CO_2 emissions. *Atmospheric Chemistry and Physics*, *20*(9), 5293–5308.

Järvi, L., Nordbo, A., Junninen, H., Riikonen, A., Moilanen, J., Nikinmaa, E., & Vesala, T. (2012). Seasonal and annual variation of carbon dioxide surface fluxes in Helsinki, Finland, in 2006–2010. *Atmospheric Chemistry and Physics*, *12*(18), 8475–8489.

Kljun, N., Calanca, P., Rotach, M., & Schmid, H. (2004). A simple parameterisation for flux footprint predictions. *Boundary-Layer Meteorology*, *112*(3), 503–523.

Kljun, N., Calanca, P., Rotach, M., & Schmid, H. P. (2015). A simple two-dimensional parameterisation for Flux Footprint Prediction (FFP). *Geoscientific Model Development*, *8*(11), 3695–3713.

Kunik, L., Mallia, D. V., Gurney, K. R., Mendoza, D. L., Oda, T., & Lin, J. C. (2019). Bayesian inverse estimation of urban CO_2 emissions: results from a synthetic data simulation over Salt Lake City, UT. *Elem Sci Anth*, *7*(1).

Lauvaux, T., Gurney, K. R., Miles, N. L., Davis, K. J., Richardson, S. J., Deng, A., . . . others (2020). Policy-relevant assessment of urban CO_2 emissions. *Environmental Science & Technology*, *54*(16), 10237–10245.

Lauvaux, T., Miles, N. L., Deng, A., Richardson, S. J., Cambaliza, M. O., Davis, K. J., . . . others (2016). High-resolution atmospheric inversion of urban CO_2 emissions during the dormant season of the Indianapolis Flux Experiment (INFLUX). *Journal of Geophysical Research: Atmospheres*, *121*(10), 5213–5236.

Leclerc, M. Y., & Foken, T. (2014). *Footprints in Micrometeorology and Ecology.* Springer.

Lee, T., & Koski, C. (2014). Mitigating global warming in global cities: comparing participation and climate change policies of C40 cities. *Journal of Comparative Policy Analysis: Research and Practice*, *16*(5), 475–492.

Lee, X., Massman, W., & Law, B. (2004). *Handbook of Micrometeorology: A guide for surface flux measurement and analysis.* Springer Science & Business Media.

Levin, I., & Karstens, U. (2007). Inferring high-resolution fossil fuel CO_2 records at continental sites from combined $^{14}CO_2$ and CO observations. *Tellus B*, *59*(2), 245–250.

Lietzke, B., Vogt, R., Feigenwinter, C., & Parlow, E. (2015). On the controlling factors for the variability of carbon dioxide flux in a heterogeneous urban environment. *International Journal of Climatology*, *35*(13), 3921–3941.

McKain, K., Wofsy, S. C., Nehrkorn, T., Eluszkiewicz, J., Ehleringer, J. R., & Stephens, B. B. (2012). Assessment of ground-based atmospheric observations for verification of greenhouse gas emissions from an urban region. *Proceedings of the National Academy of Sciences*, *109*(22), 8423–8428.

Menzer, O., & McFadden, J. P. (2017). Statistical partitioning of a three-year time series of direct urban net CO_2 flux measurements into biogenic and anthropogenic components. *Atmospheric Environment*, *170*, 319–333.

Miles, N. L., Richardson, S. J., Lauvaux, T., Davis, K. J., Balashov, N. V., Deng, A., ... others (2017). Quantification of urban atmospheric boundary layer greenhouse gas dry mole fraction enhancements in the dormant season: results from the Indianapolis Flux Experiment (INFLUX). *Elem Sci Anth*, *5*.

Miller, J. B., Lehman, S. J., Montzka, S. A., Sweeney, C., Miller, B. R., Karion, A., ... others (2012). Linking emissions of fossil fuel CO_2 and other anthropogenic trace gases using atmospheric $^{14}CO_2$. *Journal of Geophysical Research: Atmospheres*, *117*(D8).

Miller, J. B., Lehman, S. J., Verhulst, K. R., Miller, C. E., Duren, R. M., Yadav, V., ... Sloop, C. D. (2020). Large and seasonally varying biospheric CO_2 fluxes in the Los Angeles megacity revealed by atmospheric radiocarbon. *Proceedings of the National Academy of Sciences*, *117*(43), 26681–26687.

Nemitz, E., Hargreaves, K. J., McDonald, A. G., Dorsey, J. R., & Fowler, D. (2002). Micrometeorological measurements of the urban heat budget and CO_2 emissions on a city scale. *Environmental Science & Technology*, *36*(14), 3139–3146.

Oda, T., Bun, R., Kinakh, V., Topylko, P., Halushchak, M., Marland, G., ... others (2019). Errors and uncertainties in a gridded carbon dioxide emissions inventory. *Mitigation and Adaptation Strategies for Global Change*, *24*(6), 1007–1050.

Olivier, J., & Janssens-Maenhout, G. (2012). CO_2 emissions from fuel combustion. *IEA CO_2 report*.

Pataki, D., Alig, R., Fung, A., Golubiewski, N., Kennedy, C., McPherson, E., ... Romero Lankao, P. (2006). Urban ecosystems and the North American carbon cycle. *Global Change Biology*, *12*(11), 2092–2102.

Pataki, D., Xu, T., Luo, Y. Q., & Ehleringer, J. R. (2007). Inferring biogenic and anthropogenic carbon dioxide sources across an urban to rural gradient. *Oecologia*, *152*(2), 307–322.

Reinmann, A. B., Smith, I. A., Thompson, J. R., & Hutyra, L. R. (2020). Urbanization and fragmentation mediate temperate forest carbon cycle response to climate. *Environmental Research Letters*, *15*(11), 114036.

Richardson, S. J., Miles, N. L., Davis, K. J., Lauvaux, T., Martins, D. K., Turnbull, J. C., ... Cambaliza, M. O. L. (2017). Tower measurement network of in-situ CO_2, CH_4 and CO in support of the Indianapolis Flux (INFLUX) Experiment. *Elem Sci Anth*, *5*.

Sargent, M., Barrera, Y., Nehrkorn, T., Hutyra, L. R., Gately, C. K., Jones, T., ... others (2018). Anthropogenic and biogenic CO_2 fluxes in the Boston urban region. *Proceedings of the National Academy of Sciences*, *115*(29), 7491–7496.

Sarmiento, D. P., Davis, K. J., Deng, A., Lauvaux, T., Brewer, A., & Hardesty, M. (2017). A comprehensive assessment of land surface-atmosphere interactions in a WRF/Urban modeling system for Indianapolis, IN. *Elem Sci Anth*, *5*.

Silva, S. J., Arellano, A. F., & Worden, H. M. (2013). Toward anthropogenic combustion emission constraints from space-based analysis of urban CO_2/CO sensitivity. *Geophysical Research Letters*, *40*(18), 4971–4976.

Staufer, J., Broquet, G., Bréon, F.-M., Puygrenier, V., Chevallier, F., Xueref-Rémy, I., ... others (2016). The first 1-year-long estimate of the Paris region fossil fuel CO_2 emissions based on atmospheric inversion. *Atmospheric Chemistry and Physics*, *16*(22), 14703–14726.

Stull, R. B. (2012). *An Introduction to Boundary Layer Meteorology.* Springer Science & Business Media.

Sugawara, H., Ishidoya, S., Terao, Y., Takane, Y., Kikegawa, Y., & Nakajima, K. (2021). Anthropogenic CO_2 emissions changes in an urban area of Tokyo, Japan, due to the COVID-19 pandemic: A case study during the state of emergency in April–May 2020. *Geophysical Research Letters*, *48*(15), e2021GL092600.

Turnbull, J., Karion, A., Davis, K. J., Lauvaux, T., Miles, N. L., Richardson, S. J., ... others (2018). Synthesis of urban CO_2 emission estimates from multiple methods from the Indianapolis Flux Project (INFLUX). *Environmental Science & Technology*, *53*(1), 287–295.

Turnbull, J., Sweeney, C., Karion, A., Newberger, T., Lehman, S. J., Tans, P. P., ... others (2015). Toward quantification and source sector identification of fossil fuel CO_2 emissions from an urban area: results from the INFLUX experiment. *Journal of Geophysical Research: Atmospheres*, *120*(1), 292–312.

Turnbull, J. C., Miller, J., Lehman, S., Tans, P., Sparks, R., & Southon, J. (2006). Comparison of $^{14}CO_2$, CO, and SF_6 as tracers for recently added fossil fuel CO_2 in the atmosphere and implications for biological CO_2 exchange. *Geophysical Research Letters*, *33*(1).

Turner, A. J., Shusterman, A. A., McDonald, B. C., Teige, V., Harley, R. A., & Cohen, R. C. (2016). Network design for quantifying urban CO_2 emissions: assessing trade-offs between precision and network density. *Atmospheric Chemistry and Physics*, *16*(21), 13465–13475.

Velasco, E., & Roth, M. (2010). Cities as net sources of CO_2: review of atmospheric CO_2 exchange in urban environments measured by eddy covariance technique. *Geography Compass*, *4*(9), 1238–1259.

Vickers, D., & Mahrt, L. (1997). Quality control and flux sampling problems for tower and aircraft data. *Journal of Atmospheric and Oceanic Technology*, *14*(3), 512–526.

Vogt, R., Christen, A., Rotach, M., Roth, M., & Satyanarayana, A. (2006). Temporal dynamics of CO_2 fluxes and profiles over a Central European city. *Theoretical and Applied Climatology*, *84*(1-3), 117–126.

Wu, D., Lin, J. C., Duarte, H. F., Yadav, V., Parazoo, N. C., Oda, T., & Kort, E. A. (2021). A model for urban biogenic CO_2 fluxes: Solar-Induced Fluorescence for Modeling Urban biogenic Fluxes (SMUrF v1). *Geoscientific Model Development*, *14*(6), 3633–3661.

Wu, K., Lauvaux, T., Davis, K. J., Deng, A., Coto, I. L., Gurney, K. R., & Patarasuk, R. (2018). Joint inverse estimation of fossil fuel and biogenic CO_2 fluxes in an urban environment: An observing system simulation experiment to assess the impact of multiple uncertainties. *Elem Sci Anth*, *6*(1).

Supporting Information for "Evaluating an emissions inventory using atmospheric CO_2 flux measurements and source partitioning in a suburban environment"

Kai Wu[1,*], Kenneth J. Davis[1,2], Natasha L. Miles[1], Scott J. Richardson[1], Thomas Lauvaux[3], Daniel P. Sarmiento[4], Nikolay V. Balashov[4], Klaus Keller[5], Jocelyn Turnbull[6,7], Kevin R. Gurney[8,9], Jianming Liang[9], Geoffrey Roest[8]

[1]Department of Meteorology and Atmospheric Science, The Pennsylvania State University, University Park, Pennsylvania 16802, United States

[2]Earth and Environmental Systems Institute, The Pennsylvania State University, University Park, Pennsylvania 16802, United States

[3]Laboratoire des Sciences du Climat et del'Environnement, CEA, CNRS, UVSQ/IPSL, Université Paris-Saclay, Orme des Merisiers, 91191 Gif-sur-Yvette Cedex, France

[4]NASA Goddard Space Flight Center, Greenbelt, Maryland 20771, United States

[5]Department of Geosciences, The Pennsylvania State University, University Park, Pennsylvania 16802, United States

[6]Rafter Radiocarbon Laboratory, GNS Science, Lower Hutt 5040, New Zealand

[7]CIRES, University of Colorado at Boulder, Boulder, Colorado 80309, United States

[8]School of Informatics, Computing and Cyber Systems, Northern Arizona University, Flagstaff, Arizona 85287, United States

[9]School of Life Sciences, Arizona State University, Tempe, Arizona 85281, United States

*now at: School of GeoSciences, The University of Edinburgh, Edinburgh, United Kingdom

Specific steps to partition anthropogenic and biogenic CO_2 flux components:

Step 1: Estimate the eddy diffusivity (K) by calculating the ratio of CO_2 flux measurements (F_{CO_2}) to the vertical gradients of CO_2 mole fractions (∇ C_{CO_2}):

$$K = -\frac{F_{CO_2}}{\nabla C_{CO_2}} \tag{1}$$

Step 2: Use the vertical gradients of CO mole fractions (∇ C_{CO}) and the estimated eddy diffusivity (K) to calculate the CO fluxes (F_{CO}):

$$F_{CO} = -K \nabla C_{CO} \tag{2}$$

Step 3: Estimate the fossil fuel CO_2 emissions ($F_{CO_2 ff}$) by combining the CO fluxes with the emissions ratio (R) of CO to CO_2ff:

$$F_{CO_2 ff} = \frac{F_{CO}}{R} \tag{3}$$

Step 4: Attribute the differences between the net flux measurements and the partitioned fossil fuel CO_2 emissions to estimate the biogenic CO_2 fluxes ($F_{CO_2 bio}$):

$$F_{CO_2 bio} = F_{CO_2} - F_{CO_2 ff} \tag{4}$$

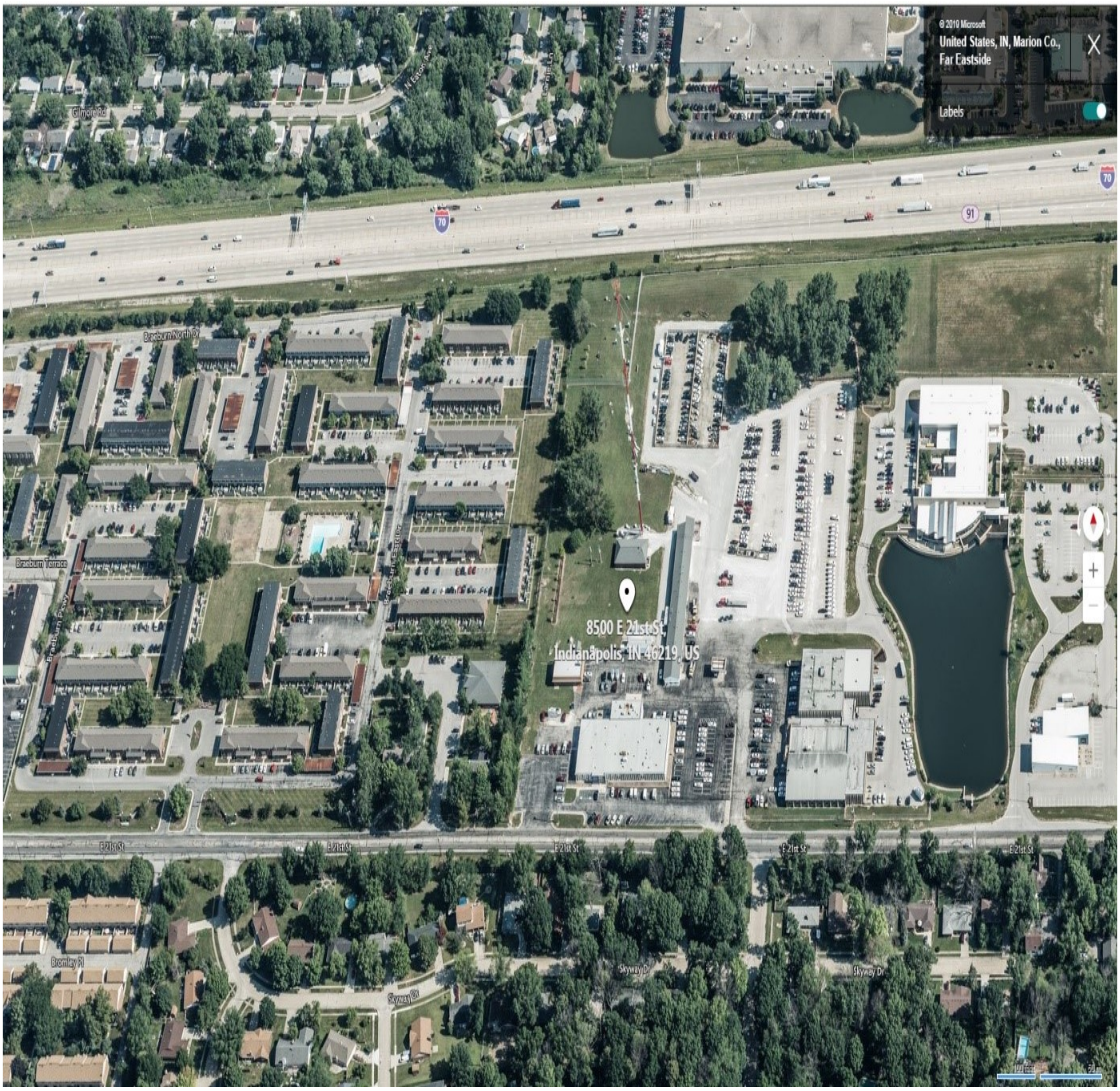

Figure S1. Surface environment around Tower 2 (39.7978°N, 86.0183°W) in Indianapolis, IN.

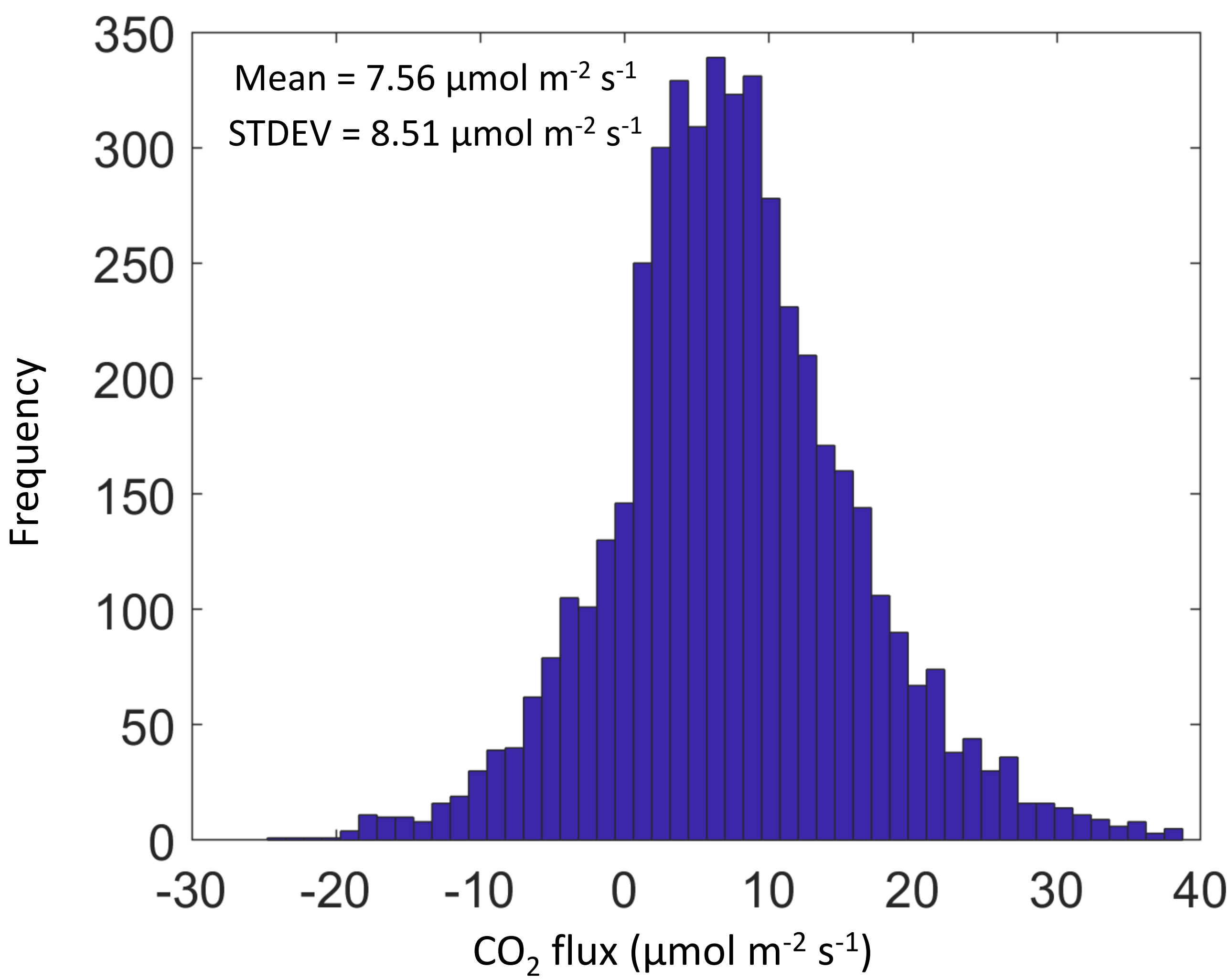

Figure S2. Histogram of eddy-covariance CO_2 flux measurements at Tower 2 from January to July in 2013.

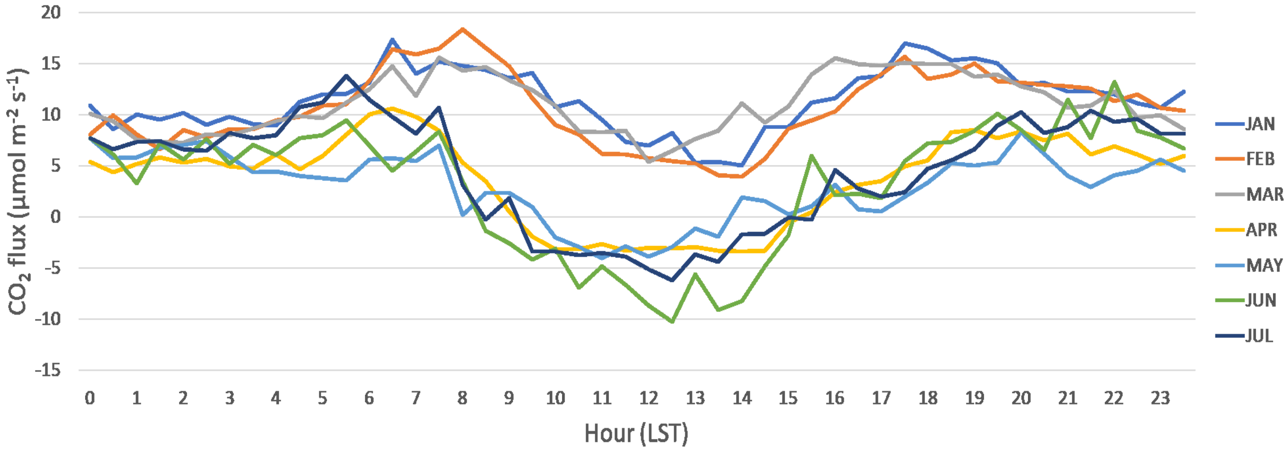

Figure S3. Diurnal variation of monthly-averaged eddy-covariance CO_2 flux measurements from January to July in 2013.

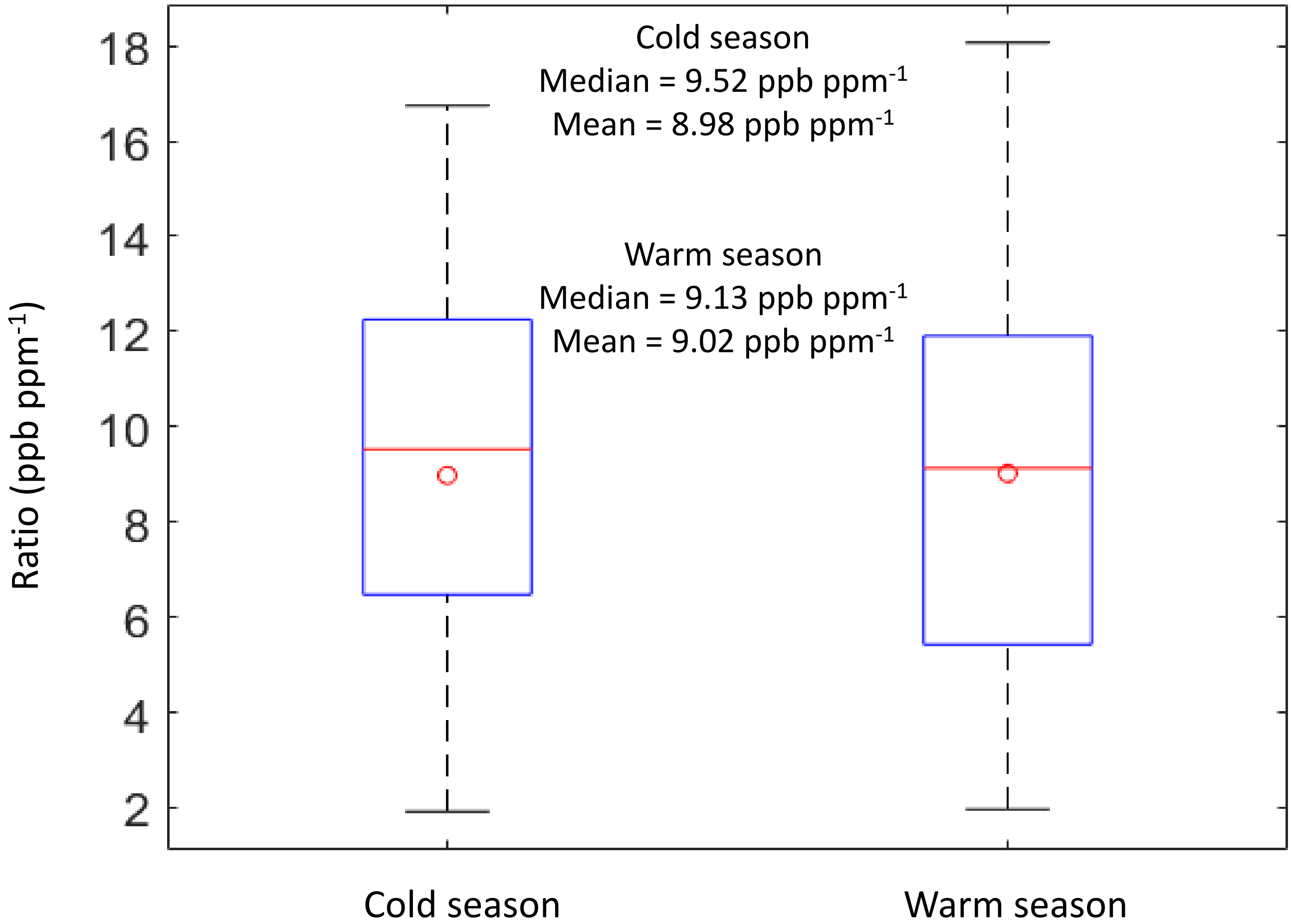

Figure S4. Ratios between the CO enhancements and the ^{14}C-based CO_2ff during the cold (JFM) and warm (AMJJ) seasons in 2013. The red circle and line mark the mean and median, respectively. The bottom and top edges of the box indicate the 25th and 75th percentiles. The whiskers extend to the most extreme data points not considered outliers that are defined as more than 1.5 times the interquartile range away from the top or bottom of the box.

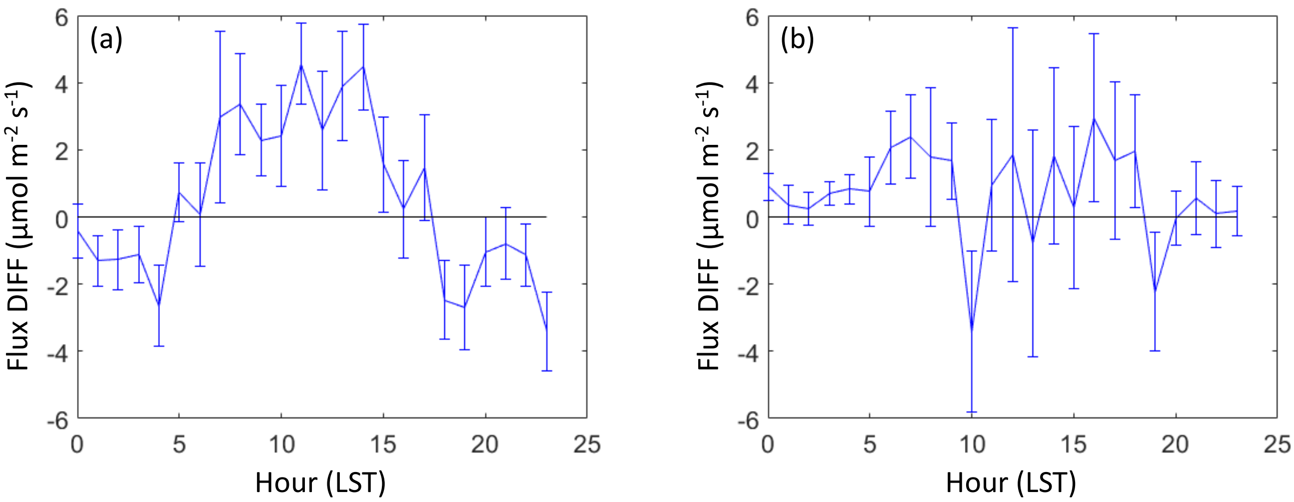

Figure S5. Diurnal variation of seasonally-averaged flux differences between the Hestia inventory and the partitioned fossil fuel CO_2 emissions (Hestia minus OBS) in the cold (JFM) (a) and warm (AMJJ) (b) seasons in 2013. Error bars are the standard errors of the seasonal means.

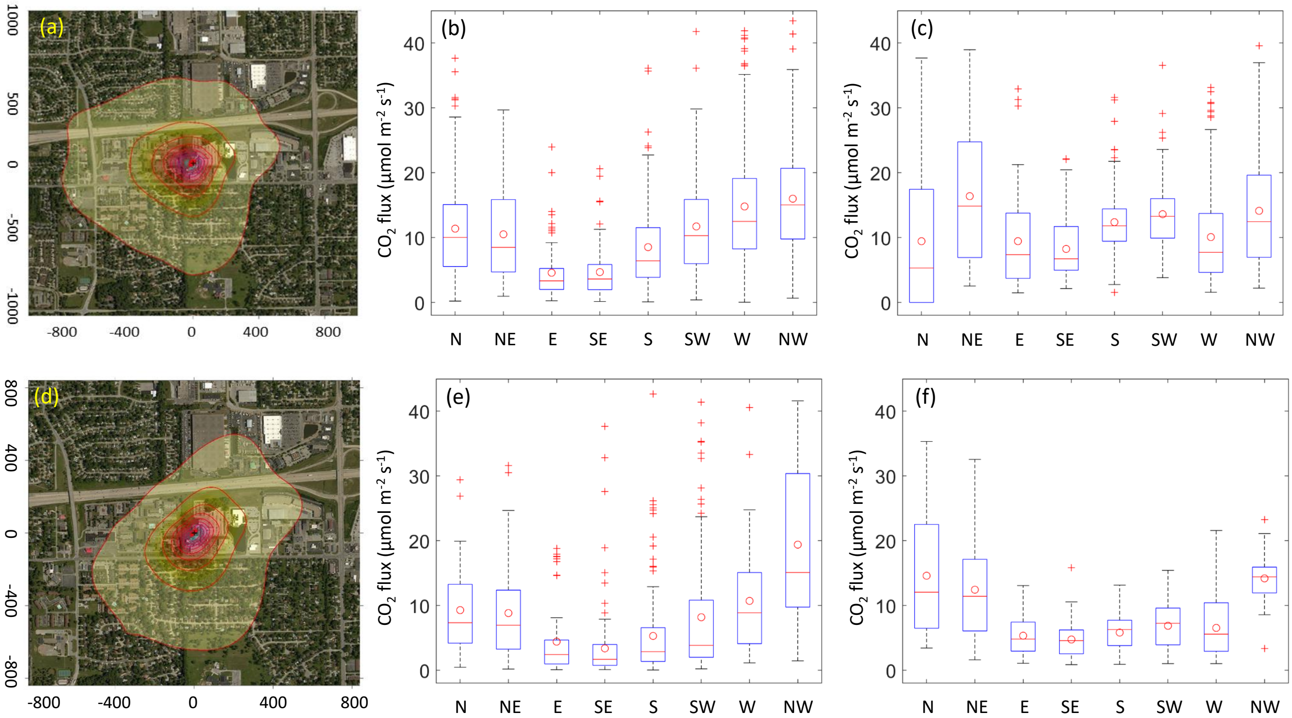

Figure S6. Cumulative flux footprints (a and d), the partitioned fossil fuel CO_2 emissions (b and e) and the Hestia inventory (c and f) for different wind directions. Panels a to c are in the cold season (JFM) and panels d to f are in the warm season (AMJJ) in 2013. The coordinates in the left panel indicate the distance (m) to the measurement site. In the middle and right panels, the red circles, the lines and the plus marks represent the mean, the median and the outliers, respectively. The bottom and top edges of the box indicate the 25th and 75th percentiles. The whiskers extend to the most extreme data points not considered outliers that are defined as more than 1.5 times the interquartile range away from the top or bottom of the box.

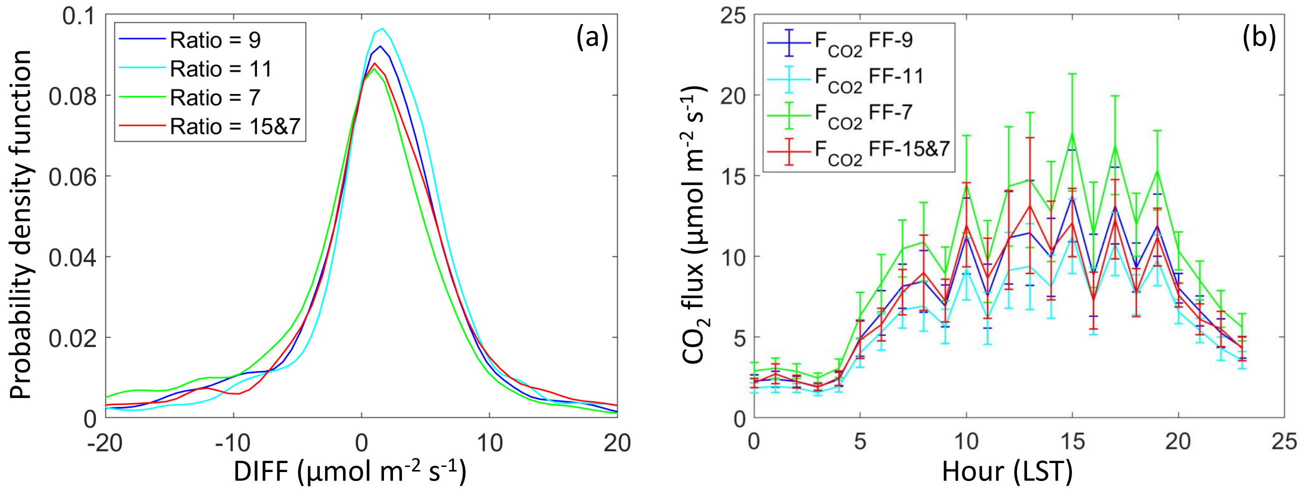

Figure S7. Probability density function of flux differences between the Hestia inventory and the partitioned fossil fuel CO_2 emissions (Hestia minus OBS) for different CO to CO_2ff emission ratios (ppb ppm^{-1}) in the warm (AMJJ) season in 2013 (a). Ratio = 15&7 represents the ratio is 15 ppb ppm^{-1} (traffic emissions) for the north wind and 7 ppb ppm^{-1} (building emissions) for other wind directions. Diurnal variation of seasonally-averaged CO_2ff fluxes for different emission ratios in the warm season (b). Error bars indicate the standard errors of the seasonal means.

Table S1. Bias (μmol m^{-2} s^{-1}), bias percentage compared to the mean partitioned CO_2ff emissions (%), and root mean square error (μmol m^{-2} s^{-1}) of the Hestia inventory for different CO to CO_2ff emissions ratios (ppb ppm^{-1}) in the warm (AMJJ) season. Ratio = 15&7 represents the ratio is 15 ppb ppm^{-1} (traffic emissions) for the north wind and 7 ppb ppm^{-1} (building emissions) for other wind directions.

Ratio	9	11	7	15 & 7
Bias	0.62	1.86	-1.34	0.77
Bias PCT[a]	9.1	33.3	-15.2	11.5
RMSE[b]	7.54	6.76	9.44	8.86

[a]percentage
[b]root mean square error